

# Temperature-dependent Raman spectroscopy in BaRuO<sub>3</sub> systems

Y. S. Lee\*

*Center for Strongly Correlated Materials Research,  
Seoul National University, Seoul 151-747, Korea*

T. W. Noh

*School of Physics and Research Center for Oxide Electronics,  
Seoul National University, Seoul 151-747, Korea*

J. H. Park and K.-B. Lee

*Department of Physics, Pohang University of Science and Technology, Pohang,  
Korea*

G. Cao<sup>†</sup> and J. E. Crow

*National High Magnetic Field Laboratory, Florida State University,  
Tallahassee, Florida 32306*

M. K. Lee and C. B. Eom

*Department of Material Science and Engineering, University of  
Wisconsin-Madison, Madison, Wisconsin 53706*

E. J. Oh and In-Sang Yang<sup>†</sup>

*Department of Physics, Ewha Womans University, Seoul 120-750, Korea  
(February 1, 2008)*

We investigated the temperature-dependence of the Raman spectra of a nine-layer BaRuO<sub>3</sub> single crystal and a four-layer BaRuO<sub>3</sub> epitaxial film, which show pseudogap formations in their metallic states. From the polarized and depolarized spectra, the observed phonon modes are assigned properly according to the predictions of group theory analysis. In both compounds, with decreasing temperature, while  $A_{1g}$  modes show a strong hardening,  $E_g$  (or  $E_{2g}$ ) modes experience a softening or no significant shift. Their different temperature-dependent behaviors could be related to a direct Ru metal-bonding through the face-sharing of RuO<sub>6</sub>. It is also observed that another  $E_{2g}$  mode of the oxygen participating in the face-sharing becomes split at low temperatures in the four layer BaRuO<sub>3</sub>. And, the temperature-dependence of the Raman continua between 250 ~ 600 cm<sup>-1</sup> is strongly correlated to the square of the plasma frequency. Our observations imply that there should be a structural instability in the face-shared structure, which could be closely related to the pseudogap formation of BaRuO<sub>3</sub> systems.

PACS number : 78.30.-j, 63.20.-e, 71.45.Lr

## I. INTRODUCTION

Recently, it was reported that a pseudogap formation can occur in 4d transition metal oxides, BaRuO<sub>3</sub> compounds.<sup>1,2</sup> Optical conductivity spectra  $\sigma_1(\omega)$  of both four-layer hexagonal (4H) BaRuO<sub>3</sub> and nine-layer rhombohedral (9R) compounds show clear electrodynamic response changes resulting from the pseudogap formation. In their metallic states, concurrent developments of a gap-like feature and a coherent mode below a gap-like feature are observed due to the partial-gap opening in the Fermi surface.

The pseudogap formations in the ruthenates could be closely related to their structures characterized by hexagonal close-packing. As shown in Fig. 1, their layered structures include the face-sharing structure of RuO<sub>6</sub> octahedra along the  $c$ -axis. In 4H and 9R struc-

tures, two and three adjacent RuO<sub>6</sub> octahedra participate in face-sharing, respectively. A direct Ru-Ru metal-bonding formed through such face-sharing distinguishes their physical properties from those of the perovskite ruthenates only with the Ru-O-Ru interaction through corner-sharing.<sup>3</sup> Actually, the metal-bonding has been seen to be closely related to interesting physical properties, such as a metal-insulator transition in Ti<sub>2</sub>O<sub>3</sub><sup>4</sup> and non-Fermi liquid behavior in La<sub>4</sub>Ru<sub>9</sub>O<sub>16</sub>.<sup>5</sup> In the case of BaRuO<sub>3</sub> systems, the quasi-one-dimensional (1D) Ru metal-bonding along the  $c$ -axis might induce a charge density wave (CDW) instability. It was reported that a 5d transition metal oxide 9R BaIrO<sub>3</sub>, which is expected to have stronger metal-bonding character than 9R BaRuO<sub>3</sub> due to a more extended 5d-orbital character, shows a static CDW instability.<sup>6</sup> For BaMO<sub>3</sub> ( $M$ =Ru, Ir) with 9R or 4H structure, it was observed that the

strength of the metal-bonding through the face-sharing should be a parameter in determining their physical properties.<sup>2</sup> These strongly indicate that a CDW instability could be related to the pseudogap formation in the BaRuO<sub>3</sub> systems.

In usual 1D density wave systems, a static CDW ordering state accompanies a structural distortion with a metal-insulator transition. When Peierls-type lattice distortion occurs, in general, new phonon modes in infrared (IR) and Raman spectra can be observed due to structural symmetry breaking. This could also result in a superlattice or an additional peak in x-ray diffraction (XRD) patterns or neutron scattering experiments. In the case of BaRuO<sub>3</sub> systems, although a 1D-like CDW instability is strongly suggested, there has been no structural report about structural distortions.<sup>7</sup> These might be related to a fluctuation-type instability without any static CDW ordering.

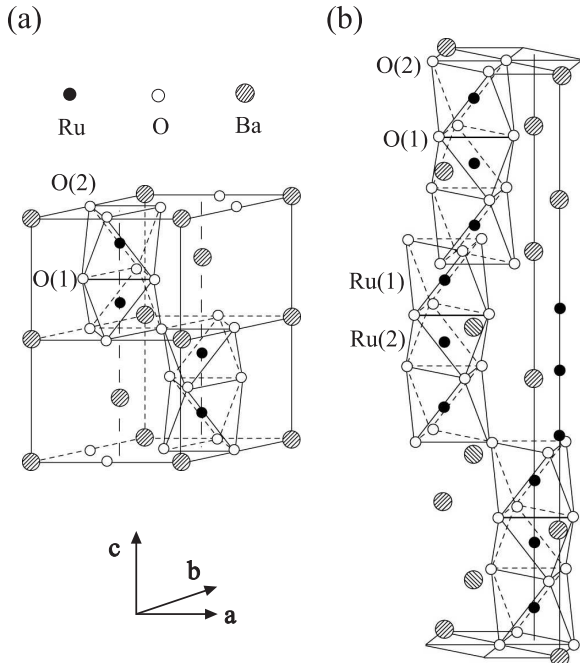


FIG. 1. Schematic diagrams of the two crystallographic forms of BaRuO<sub>3</sub>; (a) 4H phase, (b) 9R phase. The arrows represent the crystallographic axes. The details are described in the text.

When the time scale of CDW fluctuations is long enough to induce a pseudogap formation in  $\sigma_1(\omega)$ , a phonon anomaly, such as the creation or splitting of a phonon, can be observed.<sup>8–11</sup> In the metallic state of BaRuO<sub>3</sub> compounds, the screening of free carriers makes the detailed analysis of IR-active phonons difficult. On the other hand, Raman spectroscopy is known to be less affected by free-carrier responses than IR spectroscopy. So, Raman spectroscopy could be a useful tool to address the origin of pseudogap formation of BaRuO<sub>3</sub> compounds in view of their structural properties.

In this paper, we report the Raman spectra of 4H and 9R BaRuO<sub>3</sub> compounds. According to group theory analysis, the observed phonon modes are properly assigned. From the temperature ( $T$ )-dependent experiments, it is observed that the  $T$ -dependent behavior of phonons strongly depends on the vibrational directions, which could be related to the structural characteristics with the face-sharing of RuO<sub>6</sub> octahedra. Interestingly, the  $E_{2g}$  mode of the face-shared oxygen in 4H BaRuO<sub>3</sub> becomes split with decreasing  $T$ . These observations indicate that there should be a structural instability due to the metal-bonding through the face-sharing of RuO<sub>6</sub> octahedra, which could be closely related to the pseudogap formation in these ruthenates.

## II. EXPERIMENTALS

4H BaRuO<sub>3</sub> epitaxial film on (111) SrTiO<sub>3</sub> substrate was fabricated by a 90° off-axis sputtering technique.<sup>12</sup> Its thickness is about 3200 Å. XRD and transmission electron microscopy reveal that the film is composed of a high quality single domain with a  $c$ -axis structure. 9R BaRuO<sub>3</sub> single crystal was prepared by a flux-melting method.<sup>13</sup> The size of the sample is 0.5×0.5×0.2 mm<sup>3</sup>. XRD measurements showed that the  $c$ -axis was pointing along the short dimension. Due to the size limitation, most Raman spectra were obtained in the  $ab$ -plane.

Raman scattering measurements were performed in the backscattering geometry using a triple Raman spectrometer (Jobin Yvon T64000). The incident laser beam was the 514.5 nm line of an Ar-ion laser and the laser power was about 3.6 mW on the sample surface. Raman spectra were measured at various  $T$  between 5 K and 650 K. Below 300 K, a continuous flow type of cryostat was used. Above 300 K, a home-made sample heating system was used. Due to the heating effect of the focused laser, the assigned temperatures in this paper could be slightly different from the actual ones on the measured sample surface. At all  $T$ , polarized and depolarized spectra were obtained and corrected by a Bose-Einstein factor. The details are described elsewhere.<sup>14</sup>

## III. RESULTS AND DISCUSSIONS

### A. Group theory analysis and phonon assignment

The 4H structure has  $D_{6h}$  symmetry,<sup>15,16</sup> and four molecular units in the primitive cell with eight Raman-active modes ( $2A_{1g} + 2E_{1g} + 4E_{2g}$ ), twelve IR-active modes ( $5A_{2u} + 7E_{1u}$ ) and eighteen silent optic modes ( $A_{2g} + A_{1u} + 3B_{1g} + 2B_{1u} + 5B_{2u} + 6E_{2g}$ ). The Raman-active modes are composed of  $E_{2g}$  of Ba,  $A_{1g}$ ,  $E_{1g}$ , and  $E_{2g}$  of Ru, and  $A_{1g}$ ,  $E_{1g}$ , and  $2E_{2g}$  of O. The point group for the 9R structure is  $D_{3d}$ ,<sup>15,16</sup> with three

molecular units in the primitive cell. A factor group analysis predicts nine Raman-active modes ( $4A_{1g} + 5E_g$ ), sixteen IR-active modes ( $7A_{2u} + 9E_u$ ), and three silent optic modes ( $2A_{1u} + A_{2g}$ ). The Raman-active modes are composed of  $A_{1g}$  and  $E_g$  of Ba,  $A_{1g}$  and  $E_g$  of Ru, and  $2A_{1g}$  and  $3E_g$  of O.

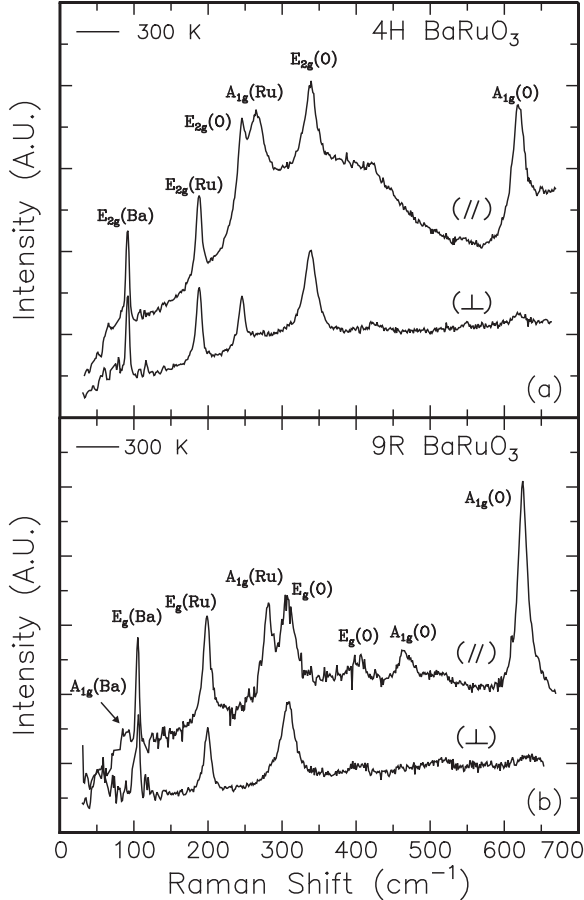


FIG. 2. Polarized (//) and depolarized ( $\perp$ ) Raman spectra of (a)  $4H$  and (b)  $9R$   $\text{BaRuO}_3$  in the  $ab$ -plane at 300 K.

It is noted that only the O ions participating in the face-sharing and only the Ru ions in  $\text{RuO}_6$  octahedra participating in the corner-sharing have Raman-active phonon modes. O ions in both ruthenates are positioned at two irreducible sites, i.e. a face-shared plane and an edge in  $\text{RuO}_6$  blocks, represented by O(1) and O(2) respectively, in Fig. 1. From the group analysis, O(2) should have only the IR-active phonon modes ( $A_{2u} + 2E_{1u}$  for  $4H$   $\text{BaRuO}_3$  and  $2A_{2u} + 3E_u$  for  $9R$   $\text{BaRuO}_3$ ), while O(1) should have both IR- and Raman-active modes. Unlike  $4H$   $\text{BaRuO}_3$ ,  $9R$   $\text{BaRuO}_3$  has two irreducible Ru-ion sites, i.e. a side and a center position in the  $\text{RuO}_6$  blocks, represented by Ru(1) and Ru(2) in Fig 1(b). Similarly to the case of O ions, Ru(2) should have the IR-active phonon modes ( $A_{2u} + E_u$ ) only. So, it is expected that  $4H$  and  $9R$   $\text{BaRuO}_3$  show similar Raman-active phonon spectra in spite of the different layered structures. For

convenience, we will abbreviate O(1) and Ru(1) to O and Ru, respectively.

Figure 2(a) shows the polarized and depolarized spectra of  $4H$   $\text{BaRuO}_3$ . Six phonon peaks are observed in the polarized spectra. In the depolarized spectra, four peaks are observed at the same frequency positions with the corresponding phonons in the polarized spectra. Note that both the  $A_{1g}$  and the  $E_{2g}$  modes in the  $D_{6h}$  symmetry contribute to the polarized signal, but only the  $E_{2g}$  modes are present in the depolarized spectra, which is an indicator for assigning the observed phonon modes.<sup>17</sup> So, four modes observed in depolarized spectra can be assigned as  $E_{2g}$  modes. Generally, the phonon frequencies related to the vibration of heavier ions are lower than those of lighter ions. Thus, the four modes in ascending order of their frequency are assigned as one  $E_{2g}(\text{Ba})$ , one  $E_{2g}(\text{Ru})$  and two  $E_{2g}(\text{O})$ . The rest of the modes in the polarized spectra are assigned as  $A_{1g}(\text{Ru})$  and  $A_{1g}(\text{O})$  from the lowest frequency. Note that according to the predictions of group theory, two  $E_{1g}$  modes of Ru and O cannot be observed in Raman spectra from the  $ab$ -plane of the thin film sample.

The observed phonons in  $9R$   $\text{BaRuO}_3$  are assigned in a similar way. As shown in Fig. 2(b), eight phonons are observed in the polarized spectra. And, three clear modes, which are assigned as  $E_g(\text{Ba})$ ,  $E_g(\text{Ru})$  and  $E_g(\text{O})$ , are observed in the depolarized spectra. Though the mode near  $403 \text{ cm}^{-1}$  in the polarized spectra is not clearly observed in the depolarized spectra at 300 K, a distinguishable feature of this mode is detected in the depolarized spectra at low  $T$ . So, the mode is assigned as another  $E_g(\text{O})$  mode. The rest of the modes in ascending order of their frequency in the polarized spectra are assigned as  $A_{1g}(\text{Ba})$  near  $85 \text{ cm}^{-1}$ ,  $A_{1g}(\text{Ru})$  near  $280 \text{ cm}^{-1}$ , and two  $A_{1g}(\text{O})$  near  $463 \text{ cm}^{-1}$  and  $625 \text{ cm}^{-1}$ . The phonon assignments of  $4H$  and  $9R$   $\text{BaRuO}_3$  are summarized in TABLE I.

On the other hand, Quilty *et al.*,<sup>18</sup> from the  $c$ -axis measurement of  $9R$   $\text{BaRuO}_3$ , assigned the  $A_{1g}(\text{Ru})$  mode at  $280 \text{ cm}^{-1}$  as another O( $E_g$ ) mode. We note, as we will discuss later, that  $T$ -dependence of this mode and its frequency are quite similar to those of the  $A_{1g}(\text{Ru})$  mode in  $4H$   $\text{BaRuO}_3$ . So, it is very likely that the mode at  $280 \text{ cm}^{-1}$  is assigned as a  $A_{1g}(\text{Ru})$  mode. It might be possible that a weak  $E_g(\text{O})$  and a strong  $A_{1g}(\text{Ru})$  mode are at nearly the same frequency.

## B. $T$ -dependent phonon spectra

Figures 3(a) and 3(b) show the  $T$ -dependent polarized spectra of  $4H$  and  $9R$   $\text{BaRuO}_3$ , respectively. The spectra are shifted up for clarity. It is observed that both compounds show similar phonon spectra. Except for the  $E_{2g}(\text{O})$  mode near  $245 \text{ cm}^{-1}$  in  $4H$   $\text{BaRuO}_3$ , five distinct phonon modes are observed at similar frequencies in both compounds. The  $A_{1g}$  and  $E_{2g}$  modes of  $4H$   $\text{BaRuO}_3$  cor-

respond to the  $A_{1g}$  and  $E_g$  modes of  $9R$  BaRuO<sub>3</sub>, respectively. It is noted that the corresponding phonon modes in both ruthenates show similar  $T$ -dependent behavior.

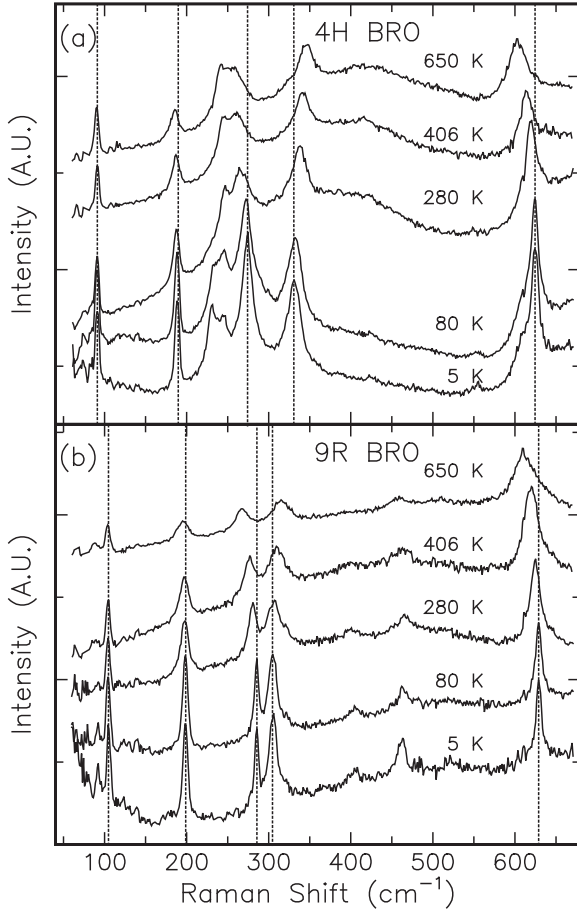


FIG. 3. Temperature-dependent polarized spectra of (a)  $4H$  and (b)  $9R$  BaRuO<sub>3</sub> in the  $ab$ -plane. The spectra are shifted up for clear presentation. The dotted lines are for guidance.

The  $A_{1g}$  modes show different  $T$ -dependent behavior from the  $E_{2g}$  ( $E_g$ ) modes in both compounds. First, the  $A_{1g}(\text{Ru})$  mode near  $620\text{ cm}^{-1}$  and the  $A_{1g}(\text{O})$  mode near  $270\text{ cm}^{-1}$  strongly shift to higher frequencies with decreasing  $T$ . [The  $A_{1g}(\text{Ba})$  mode in  $9R$  BaRuO<sub>3</sub> shows a relatively weak hardening.] On the contrary, the  $E_{2g}(\text{O})$  mode in  $4H$  BaRuO<sub>3</sub> near  $340\text{ cm}^{-1}$  and the  $E_g(\text{O})$  mode in  $9R$  BaRuO<sub>3</sub> near  $300\text{ cm}^{-1}$  show a strong softening at lower  $T$ . These softenings are quite unusual in that the general  $T$ -dependent behavior of phonons is to show a hardening at lower  $T$  due to an anharmonicity of lattice vibrations. Even in a quite wide  $T$  variation by  $\sim 650\text{ K}$ , the  $E_{2g}(\text{Ba}, \text{Ru})$  mode in  $4H$  BaRuO<sub>3</sub> and  $E_g(\text{Ba}, \text{Ru})$  mode in  $9R$  BaRuO<sub>3</sub> show a very small change. On the other hand, as shown in Fig. 3(b), another  $E_{2g}(\text{O})$  mode near  $245\text{ cm}^{-1}$ , which is present only in the  $4H$  BaRuO<sub>3</sub>, shows an anomalous  $T$ -dependence. This mode splits into two modes at low  $T$ . [The details will be discussed

in the next section.]

Figure 4 shows the detailed  $T$ -dependence of the phonons. The left panels, Figs. 4 (a), (b), (c), and (d) show the  $T$ -dependences of the  $A_{1g}(\text{O})$ ,  $E_{2g}(\text{O})$ ,  $A_{1g}(\text{Ru})$ , and  $E_{2g}(\text{Ru})$  modes, respectively, of  $4H$  BaRuO<sub>3</sub>. The right panels, Figs. 4 (e), (f), (g), and (h) show the  $T$ -dependence of the phonons of  $9R$  BaRuO<sub>3</sub> corresponding to those of  $4H$  BaRuO<sub>3</sub>, in sequence. While  $A_{1g}(\text{O})$  modes show strong hardenings,  $E_{2g}(\text{O})$  (or  $E_g$ ) modes show softenings with decreasing  $T$ . Similarly,  $A_{1g}(\text{Ru})$  modes show strong hardenings, but no significant change of  $E_{2g}(\text{Ru})$  (or  $E_g$ ) modes is observed. It is clear that  $A_{1g}$  modes show different  $T$ -dependent behavior from  $E_{2g}$  ( $E_g$ ) modes.<sup>19</sup>

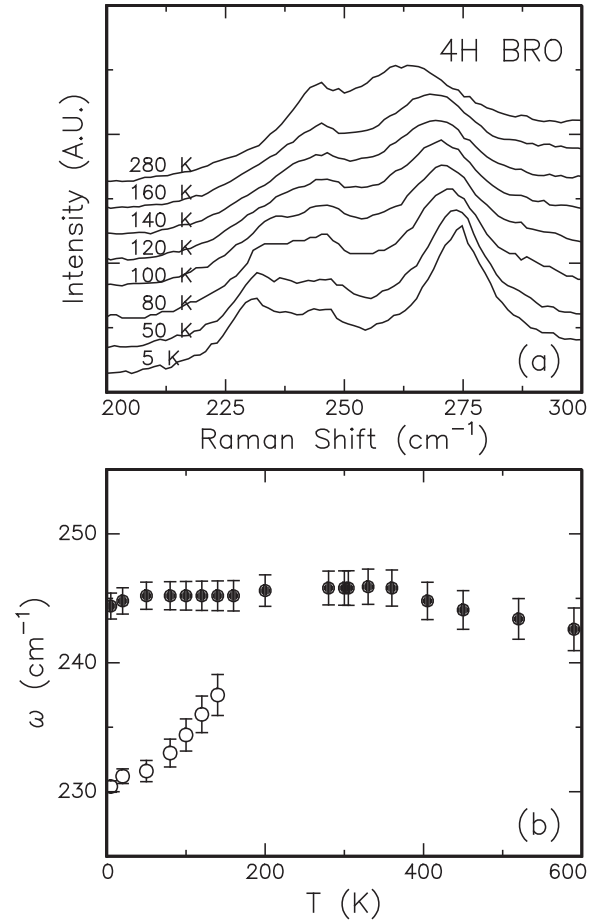


FIG. 4. The temperature-dependence of the phonon frequencies of (a)  $A_{1g}(\text{O})$ , (b)  $E_{2g}(\text{O})$ , (c)  $A_{1g}(\text{Ru})$ , and (d)  $E_{2g}(\text{Ru})$  in  $4H$  BaRuO<sub>3</sub>. (e)  $A_{1g}(\text{O})$ , (f)  $E_g(\text{O})$ , (g)  $A_{1g}(\text{Ru})$ , and (h)  $E_g(\text{Ru})$  in  $9R$  BaRuO<sub>3</sub>.

It is noted that the  $T$ -dependent behavior of the phonon modes closely depends on the direction of lattice vibrations. As a tentative description,  $E_g$  (or  $E_{2g}$ ) and  $A_{1g}$  modes are related to the vibrations in the  $ab$ -plane and along the  $c$ -axis, respectively. The different  $T$ -dependence of the  $A_{1g}$  and  $E_{2g}$  (or  $E_g$ ) modes could originate from their anisotropic structural properties with the

face-sharing of  $\text{RuO}_6$  octahedra along the  $c$ -axis, through which a strong anisotropic interaction, i.e. a direct Ru metal-bonding, occurs.

The strong hardenings of  $A_{1g}$  modes indicate that the bonding stiffness along the  $c$ -axis becomes larger. This also implies that the interaction along the  $c$ -axis, i.e. a direct Ru metal-bonding, becomes stronger. It is noted that strong hardenings of  $A_{1g}$  modes cannot be simply explained by the variation of the  $c$ -axis lattice constant  $c$ . The  $A_{1g}$  modes vibrating along the  $c$ -axis are expected to have a close relation with  $c$ . However, while synchrotron XRD experiments with  $4H$   $\text{BaRuO}_3$  report that its  $c$  is changed just by  $\sim 0.005$  Å with  $T$  varying between 30 K and 310 K,<sup>20</sup> the phonon frequency  $\omega_{ph}$  of the  $A_{1g}$  modes is changed by  $\sim 10$   $\text{cm}^{-1}$  in the corresponding  $T$  range. These changes of the  $\omega_{ph}(A_{1g})$  are much larger than those of the cuprates, where the stretching modes in Cu-O planes are quite sensitive to Cu-O bonding distances; while the lattice constant in the  $ab$ -plane is reduced by about 0.1 Å, the  $\omega_{ph}$  increases higher by 100  $\text{cm}^{-1}$ .<sup>21</sup> The relatively large change of the  $\omega_{ph}(A_{1g})$  in  $\text{BaRuO}_3$  systems means that there must be another electronic contribution to the strong hardening of the  $A_{1g}$  modes in addition to those of the lattice effect.<sup>22</sup> It is noted that similar hardening of the phonon modes in some manganites are observed due to charge ordering fluctuation.<sup>23</sup> On the other hand, in the infinite 1D chain cuprates, i.e.  $\text{Ca}_{2-x}\text{Sr}_x\text{CuO}_3$ , Drechsler *et al.* suggested the possible existence of a dynamic Peierl-type distortion and predicted phonon anomalies such as a hardening or a splitting.<sup>24</sup> The strong hardenings of the  $A_{1g}$  modes in the 1D-like ruthenates might be related to the CDW fluctuation by the metal-bonding.

Unlike the  $A_{1g}$  modes,  $E_{2g}$  (or  $E_g$ ) modes vibrating normally to the metal bonding direction show softenings or no significant change. Especially, strong softenings of the  $E_{2g}(\text{O})$  (or  $E_g$ ) modes are quite unusual. It is noted that only the oxygens participating in the face-sharing have Raman-active modes. So, the softenings of the  $E_{2g}(\text{O})$  (or  $E_g$ ) modes indicate that the bonding stiffness among the face-shared oxygens reduces and that there should be a kind of structural instability in the face-shared O structure. This also implies that the Ru-O-Ru interaction weakens as a Ru-Ru interaction strengthens, which could induce the stronger 1D-character. These differences in  $T$ -dependence between  $A_{1g}$  and  $E_g$  ( $E_{2g}$ ) modes in  $\text{BaRuO}_3$  could be a unique feature reflecting a structural instability due to the increase of the metal-bonding strength.<sup>25</sup>

### C. Splitting of $E_{2g}(\text{O})$ mode in $4H$ $\text{BaRuO}_3$

Another important observation is that the  $E_{2g}(\text{O})$  mode near 245  $\text{cm}^{-1}$  in  $4H$   $\text{BaRuO}_3$  shows a clear splitting. It is noted that this  $E_{2g}(\text{O})$  mode is not permitted in  $9R$   $\text{BaRuO}_3$  from group theory analysis. As shown

in Fig. 5(a), as  $T$  decreases, the  $E_{2g}(\text{O})$  mode becomes suppressed and a new mode at lower frequency develops. Together with the softenings of other  $E_{2g}(\text{O})$  modes, this splitting clearly indicates the existence of a structural instability in the face-shared structure. While the onset temperature of the phonon splitting is not clear, as shown in Fig 5(b), some anomaly is observed at  $\sim 360$  K, where the  $T$ -dependence of the  $E_{2g}(\text{O})$  mode is changed. This appears consistent with the optical observation that the pseudogap feature is still observed at 300 K.<sup>2</sup> It is very likely that this structural instability is closely related to the origin of the pseudogap formation in the ruthenates, i.e. the CDW instability.

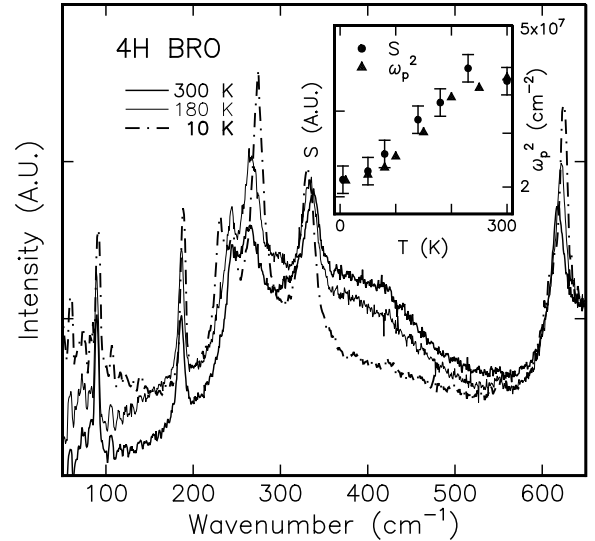


FIG. 5. (a) Temperature-dependent behavior of  $E_{2g}(\text{O})$  mode in  $4H$   $\text{BaRuO}_3$ . (b) Phonon frequency vs. temperature. The solid and open circle symbols represent the  $E_{2g}(\text{O})$  mode and a new phonon mode, respectively.

It is noted that the phonon splitting happens in the  $E_{2g}(\text{O})$  mode vibrating normally to the metal-bonding direction. The splitting of an IR-active phonon mode in the  $ab$ -plane was also observed for a static CDW  $9R$   $\text{BaIrO}_3$ .<sup>6</sup> This implies that the charge modulation along the  $c$ -axis might be closely related to the structural instability in the  $ab$ -plane. On the other hand, it is interesting that only the  $E_{2g}(\text{O})$  mode near 245  $\text{cm}^{-1}$  shows the splitting. This means that the local structural distortion related to this mode occurs, maintaining the total crystallographic symmetry of the  $4H$  compound. More theoretical and experimental studies are needed to understand the unusual CDW instability and its detailed relation to the pseudogap formation.

### D. Electronic Raman continua

Electronic Raman continua give important information about the electronic excitation. Figure 6 shows  $T$ -

dependent polarized spectra of  $4H$  BaRuO<sub>3</sub>. As  $T$  decreases, Raman continua below  $200\text{ cm}^{-1}$  increase. This behavior is commonly observed in polarized and depolarized spectra in both ruthenates. The increase of Raman continua in low frequency region could be due to the reduction of the screening of free carriers on elastic scatterings, such as Rayleigh responses. This is consistent with optical observations that a reduction of carrier density  $n$  occurs with pseudogap formation.<sup>1,2</sup> Similar behavior was observed in some perovskite manganites with the metal-insulator transition.<sup>26</sup>

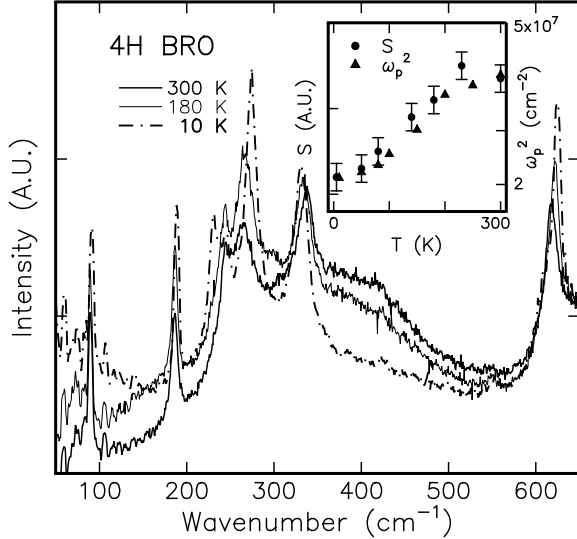


FIG. 6. Temperature-dependent Raman spectra of the  $4H$  BaRuO<sub>3</sub> in the polarized direction. Inset: the solid circle and the solid triangle symbols represent the integrated Raman backgrounds  $S$  and the square of the plasma frequency  $\omega_p^2$  (quoted from Ref. [2]).

Another important point is that a broad Raman continuum near  $400\text{ cm}^{-1}$  in  $4H$  BaRuO<sub>3</sub> is observed with a significant  $T$ -dependence.<sup>27</sup> As shown in Fig. 6, this broad continuum becomes suppressed with decreasing  $T$ . Because the maximum of the continuum is at a relatively high frequency, it cannot be an electronic Raman scattering by charge fluctuations arising from electron-hole excitations near the Fermi energy.<sup>28</sup> And, its position is different from that of the pseudogap position,  $\sim 650\text{ cm}^{-1}$ .<sup>2</sup> To get qualitative physical insights, we integrated the Raman backgrounds in the frequency region of  $250 \sim 600\text{ cm}^{-1}$ , where the  $T$ -dependence is dominant.<sup>29</sup> Interestingly, as shown in the inset of Fig. 6, the integrated area  $S$  is strongly correlated with the square of the plasma frequency  $\omega_p^2$ , obtained by optical measurement.<sup>2</sup> The reduction in  $\omega_p^2$  originates mainly from a reduction in  $n$  caused by a partial-gap opening on the Fermi surface. The strong correlation between  $S$  and  $\omega_p^2$  indicates that the suppression of the distinct Raman excitation near  $400\text{ cm}^{-1}$  might be closely related to the pseudogap formation.

#### IV. SUMMARY

Raman spectra in  $4H$  and  $9R$  BaRuO<sub>3</sub> show interesting features related to the metal-bonding formed through the face-sharing of RuO<sub>6</sub> octahedra. The temperature-dependence of the observed phonons strongly depend on the vibration direction with respect to the metal-bonding. For  $4H$  BaRuO<sub>3</sub>, another  $E_{2g}$  mode of the oxygen participating in the face-sharing is split clearly. The temperature-dependence of the broad electronic Raman continua near  $400\text{ cm}^{-1}$  suggests a partial-gap opening on the Fermi surface. These observations indicate that there occurs a kind of structural instability due to the metal-bonding, which could be closely related to the pseudogap formation in the BaRuO<sub>3</sub> systems.

#### ACKNOWLEDGMENTS

We acknowledge Jaejun Yu at Seoul National University for his helpful discussions. This work was supported by KOSEF through CSCMR. TWN acknowledges Ministry of Science and Technology for financial supports through the Creative Research Initiative program. EJO and ISY acknowledge the support from the grant (No. KRF2000-015-DS0014) of Basic Science Research Institute program of the Korea Research Foundation.

\* e-mail: yslee@phy.snu.ac.kr

† Present address: Department of Physics and Astronomy, University of Kentucky, Lexington, KY 40506.

‡ Corresponding author, e-mail: yang@mm.ewha.ac.kr

<sup>1</sup> Y. S. Lee, J. S. Lee, K. W. Kim, T. W. Noh, Jaejun Yu, E. J. Choi, G. Cao, and J. E. Crow, *Europhys. Lett.* **55**, 280 (2001).

<sup>2</sup> Y. S. Lee, J. S. Lee, K. W. Kim, T. W. Noh, Jaejun Yu, Yunkyu Bang, M. K. Lee, and C. B. Eom, *Phys. Rev. B* **64**, 165109 (2001).

<sup>3</sup> J.T. Rijssenbeek, R. Jin, Yu. Zadorozhny, Y. Liu, B. Batlogg, and R.J. Cava, *Phys. Rev. B* **59**, 4561 (1999).

<sup>4</sup> P. A. Cox, *Transition metal oxides* (Clarendon press, Oxford, 1992).

<sup>5</sup> P. Khalifah, K. D. Nelson, R. Jin, Z. Q. Mao, Y. Liu, Q. Huang, X. P. A. Gao, A. P. Ramirez, and R. J. Cava, *Nature (London)*, **411**, 669 (2001).

<sup>6</sup> G. Cao, J. E. Crow, R. P. Guertin, P. F. Henning, C. C. Homes, M. Strongin, D. N. Basov, and E. Lochner, *Solid State Commun.* **113**, 657 (2000).

<sup>7</sup> Recent synchrotron X-ray diffraction experiments with the  $c$ -axis oriented  $4H$  BaRuO<sub>3</sub> epitaxial film report no superlattice peak. [Ref. 20]

<sup>8</sup> Y. S. Lee, T. W. Noh, H. S. Choi, E. J. Choi, H. Eisaki, and S. Uchida, *Phys. Rev. B* **62**, 5285 (2000).

- <sup>9</sup> G. Blumberg, M. V. Klein, and S.-W. Cheong, Phys. Rev. Lett. **80**, 564 (1998).
- <sup>10</sup> Y. Lin and J. E. Eldridge, Phys. Rev. B **58**, 3477 (1998).
- <sup>11</sup> D. N. Argyriou, H. N. Bordallo, B. J. Campbell, A. K. Cheetham, D. E. Cox, J. S. Gardner, K. Hanif, A. dos Santos, and G. F. Strouse, Phys. Rev. B **61**, 15269 (2000).
- <sup>12</sup> M. K. Lee, C. B. Eom, W. Tian, X. Q. Pan, M. C. Smoak, F. Tsui, and J. J. Krajewski, Appl. Phys. Lett. **77**, 364 (2000).
- <sup>13</sup> M. Shepard, S. McCall, G. Cao, and J. E. Crow, J. Appl. Phys. **81** 4978 (1997).
- <sup>14</sup> J. Y. Kim, S. Y. Lee, I. S. Yang, T. G. Lee, S. S. Yom, K. Kim, J. H. Kim, Physica C **308**, 60 (1998).
- <sup>15</sup> P. C. Donohue, L. Katz, and R. Ward, Inorganic Chemistry **4**, 306 (1965).
- <sup>16</sup> P. C. Donohue, L. Katz, and R. Ward, Inorganic Chemistry **5**, 335 (1966).
- <sup>17</sup> M. Cardona and G. Güntherodt, *Light scattering in Solids II* (Springer-Verlag, Berlin, Heidelberg, New York, 1982).
- <sup>18</sup> J. Quilty, H. J. Trodahl, and A. Edgar, Solid State Commun. **86**, 369 (1993).
- <sup>19</sup> Most of the phonon modes don't show any distinguishable anomaly in their width parameters, but instead a normal sharpening due to the reduction of a thermal fluctuation with decreasing  $T$ .
- <sup>20</sup> J. H. Park, K. B. Lee, M. K. Lee, and C. B. Eom, to be published.
- <sup>21</sup> S. Tajima, T. Ido, S. Ishibashi, T. Itoh, H. Eisaki, Y. Mizuo, T. Arima, H. Takagi, and S. Uchida, Phys. Rev. B **43**, 10496 (1991).
- <sup>22</sup> K. H. Kim, J. Y. Gu, H. S. Choi, G. W. Park, and T. W. Noh, Phys. Rev. Lett. **77**, 1877 (1996).
- <sup>23</sup> H. J. Lee, K. H. Kim, J. H. Jung, T. W. Noh, R. Suryanarayanan, G. Dhalenne, and A. Revcolevschi, Phys. Rev. B **62**, 11320 (2000).
- <sup>24</sup> S.-L. Drechsler, J. Malek, M. Y. Lavrentiev, and H. Köppel, Phys. Rev. B **49**, 233 (1994).
- <sup>25</sup> The previous optical studies suggested that  $T^*$  should be  $\sim 430$  K for 9R BaRuO<sub>3</sub> and above 300 K for 4H BaRuO<sub>3</sub>. In our Raman spectra, weak anomalies in the  $T$  region of 350 K  $\sim$  450 K are observed in both BaRuO<sub>3</sub> materials.
- <sup>26</sup> S. Yoon, H. L. Liu, G. Schollerer, S. L. Cooper, P. D. Han, D. A. Payne, S.-W. Cheong, Z. Fisk, Phys. Rev. B **58**, 2795 (1998).
- <sup>27</sup> This electronic background is observed only in polarized spectra. This indicates that the Raman excitation might be related to an intraband transition within the conduction Ru 4d band. This background is hardly observed in 9R BaRuO<sub>3</sub> with a smaller  $n$  than 4H BaRuO<sub>3</sub>.
- <sup>28</sup> M. V. Klein and S. B. Dierker, Phys. Rev. B **29**, 4976 (1984).
- <sup>29</sup> It is assumed that the intensities of the phonons are not changed with  $T$  variation.

TABLE I. Summaries of the Raman-active phonon modes in 4H and 9R BaRuO<sub>3</sub> at 300 K.

4H BaRuO <sub>3</sub>			9R BaRuO <sub>3</sub>		
mode	frequency (cm <sup>-1</sup> )	assignment	mode	frequency (cm <sup>-1</sup> )	assignment
			$A_{1g}$	85	Ba
$E_{2g}$	91	Ba	$E_g$	105	Ba
$E_{2g}$	187	Ru	$E_g$	199	Ru
$E_{2g}$	245	O			
$A_{1g}$	264	Ru	$A_{1g} (E_g)$	282	Ru (C)
$E_{2g}$	339	O	$E_g$	307	O
			$E_g$	403	O
			$A_{1g}$	463	O
$A_{1g}$	619	O	$A_{1g}$	625	O